

This discussion paper is/has been under review for the journal The Cryosphere (TC).  
Please refer to the corresponding final paper in TC if available.

# Statistical adaptation of ALADIN RCM outputs over the French alpine massifs – application to future climate and snow cover

M. Rousselot, Y. Durand, G. Giraud, L. Mérindol, I. Dombrowski-Etchevers, and M. Déqué

Météo-France/CNRS, CNRM-GAME URA 1357, France

Received: 6 December 2011 – Accepted: 20 December 2011 – Published: 19 January 2012

Correspondence to: M. Rousselot (marie.rousselot@gmail.com)

Published by Copernicus Publications on behalf of the European Geosciences Union.

TCD

6, 171–210, 2012

## Statistical adaptation of ALADIN RCM

M. Rousselot et al.

Title Page

Abstract

Introduction

Conclusions

References

Tables

Figures

◀

▶

◀

▶

Back

Close

Full Screen / Esc

Printer-friendly Version

Interactive Discussion



## Abstract

In this study, snowpack scenarios are modelled across the French Alps using dynamically downscaled variables from the ALADIN Regional Climate Model (RCM) for the control period (1961–1990) and three emission scenarios (SRES B1, A1B and A2) by the mid- and late of the 21st century (2021–2050 and 2071–2100). These variables are statistically adapted to the different elevations, aspects and slopes of the alpine massifs. For this purpose, we use a simple analogue criterion with ERA40 series as well as an existing detailed climatology of the French Alps (Durand et al., 2009a) that provides complete meteorological fields from the SAFRAN analysis model. The resulting scenarios of precipitation, temperature, wind, cloudiness, longwave and shortwave radiation, and humidity are used to run the physical snow model CROCUS and simulate snowpack evolution over the massifs studied. The seasonal and regional characteristics of the simulated climate and snow cover changes are explored, as is the influence of the scenarios on these changes. Preliminary results suggest that the Snow Water Equivalent (SWE) of the snowpack will decrease dramatically in the next century, especially in the Southern and Extreme Southern part of the Alps. This decrease seems to result primarily from a general warming throughout the year, and possibly a deficit of precipitation in the autumn. The magnitude of the snow cover decline follows a marked altitudinal gradient, with the highest altitudes being less exposed to climate change. Scenario A2, with its high concentrations of greenhouse gases, results in a SWE reduction roughly twice as large as in the low-emission scenario B1 by the end of the century. This study needs to be completed using simulations from other RCMs, since a multi-model approach is essential for uncertainty analysis.

## 1 Introduction

In the Alps, snow is a natural water storage component and a major source of income for the tourist industry. Snow cover reduction may have important environmental and socio-economic impacts on water resources, winter tourism, ecology and local

TCD

6, 171–210, 2012

## Statistical adaptation of ALADIN RCM

M. Rousselot et al.

Title Page

Abstract

Introduction

Conclusions

References

Tables

Figures

◀

▶

◀

▶

Back

Close

Full Screen / Esc

Printer-friendly Version

Interactive Discussion



changes in climate. In a context of global warming, an essential prerequisite is thus to understand the links between climate and snow cover for present and future periods.

Long-term climatology has been established for about the last half of the 20th century throughout the Alps on the basis of observations or reanalyses for (Latarnser and Schneebeli, 2003), France (Martin and Etchevers, 2005; Durand et al., 2009a,b), Austria (Hantel et al., 2000; Schöner et al., 2000) and Italy (Acquaotta et al., 2009). These studies suggest that, since the early 1980's, snow cover has been substantially and rapidly reduced in most of the low and mid-altitude areas. Simultaneously, temperature has largely increased, at a rate often much faster than on the global scale (Schöner et al., 2000; Beniston et al., 2003; Durand et al., 2009a). In contrast, evidence for precipitation trends is not clear, showing either a slight increase in winter and a decline in summer, as in the Swiss Alps (Frei and Schär, 1998; Beniston et al., 2003), or no significant trend, as in the French Alps (Durand et al., 2009a).

Concerning future snow evolution, first estimations have been obtained through simple extrapolations of current observed trends (e.g., Beniston et al., 2003) or simple sensitivity studies with snow models (Martin et al., 1994; Latarnser and Schneebeli, 2003). Other attempts have been made to obtain more detailed scenarios of snow cover derived from physically-coherent climate scenarios (Martin et al., 1997). However, the main obstacle to many climate impact studies, in particular future snow cover modelling, is strongly related to the difficulty of modelling climate at relevant spatial scales. Most of the 21st century climate projections made in recent years have relied on climate scenarios from global climate models (GCMs). However, the typical scale of these models (300–150 km) is very insufficient for most impact studies, particularly when working in mountain areas, where a much higher resolution is required to properly resolve the topography. Therefore, so-called downscaling techniques, often categorized into statistical and dynamical approaches, have been developed. We present these approaches briefly here; they are reviewed in e.g., Maraun et al. (2010b).

TCO

6, 171–210, 2012

## Statistical adaptation of ALADIN RCM

M. Rousselot et al.

Title Page

Abstract

Introduction

Conclusions

References

Tables

Figures

◀

▶

◀

▶

Back

Close

Full Screen / Esc

Printer-friendly Version

Interactive Discussion



**Statistical adaptation  
of ALADIN RCM**

M. Rousselot et al.

Title Page

Abstract

Introduction

Conclusions

References

Tables

Figures

◀

▶

◀

▶

Back

Close

Full Screen / Esc

Printer-friendly Version

Interactive Discussion



In the first downscaling approach, statistical links are determined between large-scale climate predictors (from observations or climate models) and local observations of the variable of interest (e.g. temperature, precipitation). There is a broad range of statistical methods of contrasting complexity, from simple regression and analogue methods to more complex weather typing and neural network approaches, together with their combinations (see review by e.g., Maraun et al., 2010b). Their common point is that they all rely on the availability and quality of observation series, which may pose problems in some mountain regions. They are also based on the hypothesis that the statistical link existing between the spatial scales in the current climate will remain valid for future changed climatic conditions. Despite these limitations, statistical methods have been extensively used in the Alps, to work on specific months (Frey-Buesset al., 1995), reconstruct recent temperature evolution (Kettle and Thompson, 2004), obtain precipitation scenarios (Schmidli et al., 2007) or study snow cover (Martin et al., 1997).

In contrast, dynamical downscaling explores the physical links between large and fine-scale atmospheric features, often by running regional climate models (RCMs) nested into GCMs. RCMs can be run at very fine resolution (e.g., 2 km for the Alps, Hohenegger et al., 2008) but, because of their high computational costs, such simulations can only cover short time periods (hours to weeks). Longer climatic simulations (typically 30 yr) are usually run at 50–25 km resolution (see European projects such as FP5-PRUDENCE, Christensen and Christensen, 2007 and FP6-ENSEMBLES, Hewitt and Griggs, 2004; Linden and Mitchell, 2009), or on a smaller domain at 10–15 km resolution (FP6-CECILIA, Farda et al., 2010 and CLAVIER, Hagemann et al., 2004; Haylock et al., 2008). Recently, other climatic simulations have been conducted over Europe at a spatial scale of 10 km (Déqué and Somot, 2008). All these studies reveal that increased model resolution generally improves the representation of the topography, the physical processes and the subgrid parametrization, and thus the RCM skill to reproduce the observed climate.

**Statistical adaptation  
of ALADIN RCM**

M. Rousselot et al.

Title Page

Abstract

Introduction

Conclusions

References

Tables

Figures

I◀

▶I

◀

▶

Back

Close

Full Screen / Esc

Printer-friendly Version

Interactive Discussion



In an ongoing project, SCAMPEI (French ANR project, 2009–2011), regional climate models are run at  $\sim 10$  km resolution to specifically study mountain climate and its impacts on the evolution of snow cover and debris flows in France. In this framework, we adopted a combined statistical-dynamical approach, in which some of these simulations were statistically associated with analysis of real observed meteorological situations in the French Alps. The aim was to obtain climate scenarios valid for snow cover modelling. For this specific application, we also ran a physical snow model. Results on climate and snow cover evolution are presented for the end of the 20th century (reference) and the periods 2021–2050 and 2071–2100, as well as for various IPCC greenhouse gas (GHG) emissions hypotheses.

The paper is organized as follows. In the next section, we describe the numerical set-up. Validation of the downscaling method and results of the simulated changes in climate and snow cover are presented in Sects. 3 and 4, respectively. These results are subsequently discussed in Sect. 5, which is followed by a general conclusion and recommendations for future research.

## 2 Numerical setup

In this study, we performed a simple analogue search over the French Alps to obtain climate series suitable for snow modelling. The analogue method uses fine-scale outputs of the ALADIN RCM and fine-scale meteorological analysis. Several experiments were carried out to validate the method and obtain future climate scenarios.

### 2.1 ALADIN outputs

ALADIN is a French RCM that was initially designed in the early 1990's as a limited area model derived from the global spectral model ARPEGE/IFS for short-range forecasting (Bubnová et al., 1995). A climate version of the model, based on the same physical parametrization as ARPEGE (Radu et al., 2008), has been validated at 50

and 25 km resolution on a domain covering Europe in the framework of the EU-FP6 projects ENSEMBLES and CECILIA. Recent works over Europe indicate that 12 km resolution greatly improves the fields simulated by ALADIN (Déqué and Somot, 2008; Colin et al., 2010).

Here, in the framework of the SCAMPEI project, we use outputs of the recent 30-yr ALADIN simulations run at a 12 km resolution. These runs cover a reference period (1961–1990) and two periods of the 21st century (2021–2050 and 2071–2100), under different hypotheses of economic development and GHG emissions (IPCC scenarios A1B, A2 and B1). The driving simulations are the same as in the FP6-CECILIA project: they consist of global ARPEGE simulations with variable resolution (50 km over France) driven by sea surface temperatures (SST) from the IPCC-AR4 contribution (Gibelin and Déqué, 2003).

## 2.2 Analogue method and snow modelling

A simple analogue method was applied on a domain centred on the French Alps and snow modelling was carried out on the alpine sub-domain (Fig. 1). Briefly, the modelling set-up, which is sketched in Fig. 2, was as follows. The analogue search was performed on atmospheric fields interpolated on a common grid (Fig. 1). Specifically, ALADIN atmospheric fields of air temperature at 2 m above ground (T2m) and 500 hPa geopotential height (Z500), available with a 6-h time step, were linked through a statistical distance to real, analogous large-scale reanalyses. These reanalyses consisted of a combination of ERA-40 fields from 1958–2002 (ECMWF, 2004) and Météo-France’s ARPEGE analysis from 2003–2008. They are referred to as “extended ERA40 fields”. The analogues that were sought each day for all the alpine massifs were thus representative of the main features of the meteorological flow over the Alps. The date series of these analogues was then used to retrieve finer real meteorological fields from a climatology recently established on the French Alps by Durand et al. (2009a), referred to as D09a below. This climatology consists of weather reanalyses, defined at the massif-scale for elevations ranging from 900–3600 m a.s.l. and considering various

### Statistical adaptation of ALADIN RCM

M. Rousselot et al.

Title Page	
Abstract	Introduction
Conclusions	References
Tables	Figures
◀	▶
◀	▶
Back	Close
Full Screen / Esc	
Printer-friendly Version	
Interactive Discussion	



orientations and slopes. It was obtained for 1958–2008 by forcing the meteorological system SAFRAN (Durand et al., 1999) with the extended ERA40 fields mentioned above and provided hourly fields of air temperature, quantity and phase of precipitation, humidity, cloudiness, horizontal wind speed, and direct and indirect solar radiation (D09a). Thus, in this method, raw, large-scale fields from the ERA40 database are not used explicitly for snow modelling.

The statistical distance, or analogue criterion, is built as follows. For each field  $X$ , unbiased seasonal anomalies  $\tilde{X}$  and seasonal standard deviation  $\sigma$  are computed at each grid point  $i$  on the 1961–1990 and the 1958–2008 periods for the ALADIN and extended ERA40 datasets, respectively. A Mahalanobis distance  $d$  (Mahalanobis, 1936) is then computed over the whole domain every 6 h following

$$d = \sqrt{\sum_{i=1}^N \frac{[\tilde{X}_{\text{ala}}(i) - \tilde{X}_{\text{era}}(i)]^2}{\sigma_{\text{ala}}(i)\sigma_{\text{era}}(i)}}, \quad (1)$$

where the subscripts ala and era refer to ALADIN and ERA40 fields, respectively, and  $N$  is the number of grid points.

Daily distances (from 06:00 UTC to 06:00 UTC the next day) are calculated on the nearsurface field T2m and the following upper-air fields: Z500, Z500 horizontal gradient (defined by its zonal and meridional components) and Z500 second spatial derivative. The analogue is determined by minimizing the sum of these distances. To account for the different topographies underlying the ALADIN and ERA40 fields, guarantee temporal coherence in the seasonal insolation and thus reproduce the main features of the current climate as well as possible, the analogue fields are corrected a posteriori by a quantile-quantile method (Déqué, 2007, see also Sect. 3) and appropriate factors.

Finally, these SAFRAN fields are used to force the CROCUS snow model (Brun et al., 1989, 1992), which computes profiles of temperature, density, liquid-water content and crystal types within the snowpack for the same elevations and orientations as those in SAFRAN and for three slopes (flat, 20° and 40°). These runs thus describe the

**Statistical adaptation of ALADIN RCM**

M. Rousselot et al.

Title Page	
Abstract	Introduction
Conclusions	References
Tables	Figures
◀	▶
◀	▶
Back	Close
Full Screen / Esc	
Printer-friendly Version	
Interactive Discussion	



Discussion Paper | Discussion Paper | Discussion Paper | Discussion Paper

snowpack evolution on the French alpine massifs (Fig. 1). This approach is similar to that of Durand et al. (2009b) (referred to as D09b hereafter), where a snow climatology is derived for 1958–2002 using D09a SAFRAN data in the forcing of CROCUS, the difference being that future climate series are treated here.

## 2.3 Experiments

A first set of experiments, which included a control (CT) and a cross (CR) experiment, were performed to test the method on present day climatology (Table 1). The CT experiment was run using the ALADIN outputs for 1961–1990. In this experiment, the resulting simulated climate may differ from the D09a one, used as a reference, either because the ALADIN predictors differ from real observed situations or because the analogues search method itself introduces some errors. To specifically verify the method, the cross experiment (CR) was run, in which the set of predictors exactly matched the large-scale features of the D09a dataset. Thus in CR, the analogue method was applied between the extended 1958–2008 ERA40 fields and the same dataset from which a moving 20-day window centred on the day of interest had been removed to avoid the selection of an analogue belonging to the same meteorological situation. Given the large size of the extended ERA40 subset (~14 000 days), it can be assumed that the mean value and variability tend to be identical for all data sets. In this set-up, a perfect analogue method would thus provide the same climatology as in the D09a study. The results of the experiments are described in the validation section (Sect. 3).

Future climate was studied through a second set of 6 experiments, corresponding to the 3 IPCC emission scenarios treated by ALADIN (IPCC, 2007) for each of the periods 2021–2050 and 2071–2100:

- the A1B scenario, which describes a future world with rapid, globalized future economic growth, the development of new, more efficient technologies, and a global population increase until mid-century with decline thereafter.

## Statistical adaptation of ALADIN RCM

M. Rousselot et al.

Title Page

Abstract

Introduction

Conclusions

References

Tables

Figures

◀

▶

◀

▶

Back

Close

Full Screen / Esc

Printer-friendly Version

Interactive Discussion



- the A2 scenario, which assumes regionally heterogeneous economic and technological development throughout the world and a continuously increasing population. This is one of the most GHG emissive IPCC scenarios.
- the B1 scenario, which assumes similar evolution of the global population to that in A1B, but with an economy dominated by services and information activities and the use of clean technologies. This scenario is the least emissive one, with GHG emissions that are stabilized before the end of the century.

The results of these experiments are presented in Sect. 4.

### 3 Validation on the control period

#### 3.1 Weather types

In its analysis scheme, SAFRAN is based on a classification of the input meteorological large-scale fields into 7 weather types (Durand et al., 1993). Here, this classification is used to evaluate the ability of the downscaling method to correctly identify these large-scale circulation patterns.

Figure 3 compares the weather type frequencies obtained over the French Alps during the period 1961–1990, resulting from the CT experiment and D09a climatology, on seasonal and annual time scales. There is good general agreement between the two annual datasets (Fig. 3a). On a seasonal time-scale, both experiments indicate that the French Alps are influenced mainly by 3 weather types in summer (types 4, 5 and 7, see upper left panel of Fig. 3) whereas other types occur in winter (Fig. 3b, d). Also, inter-seasonal large-scale features are similar in spring and autumn (Fig. 3c, e). The main discrepancies between the two experiments concern the frequency of strong anticyclones (type 7), which is underestimated by CT in all seasons except summer, and the summer heavy precipitation (type 4), which is systematically less frequent in CT.

Title Page

Abstract

Introduction

Conclusions

References

Tables

Figures

◀

▶

◀

▶

Back

Close

Full Screen / Esc

Printer-friendly Version

Interactive Discussion



## 3.2 Air temperature and precipitation

The degree of reliability of the analogue method in reproducing the reference D09a climate on the 1961–1990 period is assessed by considering statistical distributions of near-surface temperature and precipitation.

Figure 4 shows the seasonal quantile-quantile (q-q) diagrams of T2m in the CT (upper row) and CR (lower row) experiments. Figure 5 illustrates similar results for precipitation. Results are presented at 1800 m a.s.l. and for 4 massifs located in the different regions of the French Alps: the Mont Blanc massif (MB) in the Northern Alps, the Grandes Rousses (GR) in the Central Alps, the Queyras (Qu) in the Southern Alps and the Ubaye (Ub) in the Extreme Southern Alps (see Fig. 1 for location). Such q-q plots provide synthetic comparisons of probability distributions and are thus useful to validate the regional and seasonal patterns of the downscaled climatology.

Results obtained for T2m suggest fairly good agreement between the D09a climatology and the ALADIN outputs treated in the CT experiment for all the selected massifs and seasons (Fig. 4a–d). As expected, this correlation is improved in the CR experiment (Fig. 4e–h), in which possible sources of errors related to the use of RCM predictors have been removed.

For precipitation, the CT climatology seems to be drier than the D09a climatology, particularly in summer (Fig. 5a–d). As for temperatures, the seasonal correlation between simulated and reference precipitation distributions is generally improved in the CR experiment (Fig. 5e–h). However, in the CT experiment, precipitation intensities are still underestimated, particularly in summer and, to a lesser extent, in autumn.

The results shown in Figs. 4 and 5 are confirmed on the annual time-scale by Table 2, which gives the annual mean values of T2m and daily precipitation for each massif together with the standard deviations, for both the CT experiment and the D09a climatology. The difference between annual mean T2m of the two datasets reaches  $\sim 0.3^\circ\text{C}$  (Chartreuse massif, Table 2), a value which is well below the intrinsic error of SAFRAN reanalysis, about  $1^\circ\text{C}$  (Durand et al., 2009a). Moreover, annual mean precipitation

TCD

6, 171–210, 2012

## Statistical adaptation of ALADIN RCM

M. Rousselot et al.

Title Page

Abstract

Introduction

Conclusions

References

Tables

Figures

◀

▶

◀

▶

Back

Close

Full Screen / Esc

Printer-friendly Version

Interactive Discussion



at 1800 m a.s.l. is underestimated by 10 % (Champsaur, Alpes Azuréennes) to ~ 20 % (Haute-Maurienne) on all massifs (Table 2). Standard deviation values shown in Table 2 also suggest that the downscaled reference ALADIN series reproduces the interannual variability of both T2m and precipitation with good confidence.

Our method thus seems to perform better for temperature than precipitation fields. A possible reason is that the latter are not explicitly taken into account in the analogy criterion. Moreover, better correlations between simulated and reference values are generally obtained in the CR rather than in the CT experiment, suggesting that the use of ALADIN instead of reference ERA40 fields as predictors introduces a supplementary error in the downscaling. This error may stem from different parametrization between the ALADIN and ERA40 models, such as the description of the topography and physical processes. In particular, the observed negative bias in precipitation may be explained by the difficulty, common in regional climate modelling, of correctly simulating convective storms that are frequent in summer over Europe. Although their impact on simulated snow cover is expected to be negligible, we choose to correct the discrepancies between the statistical distributions of the D09a (reference) and CT (simulated) climatologies with a quantile-quantile method (Déqué, 2007). This approach is often used to correct RCM bias (e.g., Boé et al., 2007; Alpert et al., 2008; Kallache et al., 2011). Here, for each SAFRAN variable, a seasonal correction is applied to each quantile of the distribution according to the massif and elevation.

### 3.3 Snow water equivalent

Maps of mean values and standard deviations of winter snow water equivalent (SWE) at 1800 m a.s.l. for the reference period 1961–1990 are shown in Fig. 6. These results were either obtained by forcing CROCUS with the climate data derived from ALADIN (CT experiment) and statistically corrected by a q-q method (Fig. 6a) or directly selected in the D09b climatology (Fig. 6b). The differences in mean SWE between downscaled and reference data is of the order of magnitude of 10 mm (Fig. 6a). This value is well below the signal variability, as standard deviations are about 10 times larger

## Statistical adaptation of ALADIN RCM

M. Rousselot et al.

Title Page

Abstract

Introduction

Conclusions

References

Tables

Figures

◀

▶

◀

▶

Back

Close

Full Screen / Esc

Printer-friendly Version

Interactive Discussion



(Fig. 6b). Thus, values of SWE at 1800 m a.s.l. derived from ALADIN fields are generally in good agreement with the D09b climatology of each massif, showing a similar decreasing north-south gradient over the Alps. Results at other elevations (not shown) also suggest that the downscaling method reproduces both mean and interannual variability of current SWE with reasonable confidence.

## 4 Changes in climate and snow cover

In this section, changes in climate and snow cover derived from the ALADIN scenarios are presented. For the sake of clarity, some results are illustrated on clusters of massifs (Northern, Central, Southern and Extreme Southern Alps, see Fig. 1) presenting similar climate characteristics, as defined in Durand et al. (2009b).

### 4.1 Changes in frequency of weather types

Figure 7 illustrates changes in weather type frequency obtained for the 2021–2050 and 2071–2100 periods with respect to the CT experiment (Fig. 3). Generally, changes are larger at the end of the century than earlier and reveal a marked influence of the greenhouse gases concentration. Thus, for the 2071–2100 period, the A2 scenario leads to changes that are generally larger than in the A1 scenario, whereas the B1 scenario leads to smoother evolutions, in agreement with changes expected on a global scale (IPCC, 2007). On the annual time-scale, our results suggest a significantly increasing frequency of large, stable anticyclones (weather type 7) at the expense of the other weather types (Fig. 7a). These synoptic evolutions over France are consistent with the expected large increase in sea level pressure over the Mediterranean sea for this period (Boé et al., 2009). On the seasonal time-scale, large anticyclones (weather type 7) seem to become more frequent in winter, spring and autumn (Fig. 7b, c, e), but sparser in summer, a season dominated by frequent north-westerly and south-westerly perturbed flows (weather type 4) (Terray et al., 2004).

## Statistical adaptation of ALADIN RCM

M. Rousselot et al.

Title Page

Abstract

Introduction

Conclusions

References

Tables

Figures

◀

▶

◀

▶

Back

Close

Full Screen / Esc

Printer-friendly Version

Interactive Discussion



## 4.2 Changes in surface temperature

Figure 8 shows the annual and seasonal T2m changes at 1800 m a.s.l. over the Northern, Central, Southern and Extreme Southern Alps (Fig. 1), for 2021–2050 (left panels) and 2071–2100 (right panels) and for all scenarios, with respect to the CT experiment.

Figure 9 shows the altitudinal gradient of the annual T2m changes for the same regions, periods and scenarios.

For all scenarios, results suggest significant warming in the Alps over the next century. Mid-century projections indicate a mean annual warming of about 1.5–2 °C (Figs. 8a and 9a–d), with the largest changes obtained for the A1B scenario. As expected, the spread of the annual mean temperature change as a function of the emission scenario increases at the end of the century, ranging from ~ 2.5–5 °C for the least (B1) and the most (A2) emissive scenarios, respectively (Figs. 8f and 9e–h).

The temperature changes simulated for each scenario and period seem relatively uniform from the Northern to the Extreme Southern Alps (Fig. 8a, b) and for the elevation range considered (Fig. 9). This is probably because our method does not add any spatial variability to the input D09a climatology, as ALADIN T2m fields are generally smooth over the French Alps (not shown). Thus, these results suggest that climate change will probably affect mean temperatures over the entire Alps, and that the future alpine climate will be characterized by an increasing north-south temperature gradient (Table 2 and Durand et al., 2009a).

There is a seasonal signature of the warming, with a winter (summer) temperature anomaly that is smaller (larger) than the annual signal. This seasonal signature is clearer at the end of the century, with winter anomalies ranging from 2 to 4 °C, and summer anomalies varying between 3 and 7 °C according to the scenario (Figs. 8g, i). Spring and autumn anomalies display similar features, with intermediate values ranging from 2 to 4.5 °C for the 2071–2100 period (Fig. 8h, j).

Title Page

Abstract

Introduction

Conclusions

References

Tables

Figures

◀

▶

◀

▶

Back

Close

Full Screen / Esc

Printer-friendly Version

Interactive Discussion



### 4.3 Precipitation changes

Figure 10 shows the annual and seasonal precipitation anomalies at 1800 m a.s.l. for the 2021–2050 and 2071–2100 periods and all scenarios. Simulated precipitation changes for both 2021–2050 and 2071–2100 are highly variable according to the scenario, season and region of the French Alps and uncertainties are much larger than for temperature. Some trends can however be identified for the end of the century. At this time, annual mean anomalies show a deficit in precipitation down to  $\sim 25\%$  for the A1B and A2 scenarios, and no significant evolution for the B1 scenario (Fig. 10f). The seasonal evolution is more contrasted, suggesting that the annual precipitation decrease simulated for the A1B and A2 scenarios is primarily due to drier summers (down to  $-55\%$  precipitation in the Extreme Southern Alps for the A2 scenario) and, to a lesser extent, autumns and springs (Fig. 10h, i, j), at least in the Southern and Extreme Southern Alps. The B1 scenario seems to be the wettest one on all regions except in winter. Interestingly, in this season, all scenarios provide similar results with no significant precipitation changes with respect to signal variability (Fig. 10g) despite likely more frequent anticyclonic situations (Fig. 7b). The regions most affected by drying seem to be located in the Southern and Extreme Southern Alps, particularly during the inter-seasons (Figs. 10h, j). Thus, the current precipitation gradient observed over the Alps, decreasing from North to South (Table 2 and Durand et al., 2009a), might be strengthened in the future. In the Southern and Extreme Southern Alps, the relative summer precipitation deficit seems to be slightly smaller than in the other regions, which might be related to wet westerly/north-westerly flows being more frequent in the future, or more frequent dry anticyclonic regimes (as suggested in Fig. 7). However, the question of the link between changes in large-scale circulation and local climate evolution would deserve deeper analysis and is outside the scope of this study.

Projections for 2021–2050 are more difficult to interpret, showing very contrasted results according to scenarios, seasons and regions. In contrast to the end of the century, only the Extreme Southern Alps seem to undergo moderate drying, of less

[Title Page](#)[Abstract](#)[Introduction](#)[Conclusions](#)[References](#)[Tables](#)[Figures](#)[◀](#)[▶](#)[◀](#)[▶](#)[Back](#)[Close](#)[Full Screen / Esc](#)[Printer-friendly Version](#)[Interactive Discussion](#)

than 10% on the annual time-scale (Fig. 10a). Seasonal changes suggest that the largest precipitation decreases, of ~ 15 to 20% are expected in autumn (Fig. 10e), in all regions for the A1B and A2 scenarios and only in the Southern and Extreme Southern massifs for the B1 scenario.

Figure 11 shows the altitudinal gradients of annual precipitation changes over the main alpine regions, for 2021–2050 and 2071–2100 and all scenarios. As for temperatures, the simulated anomalies in precipitation do not seem to depend on the altitude, so the orographic gradient currently observed in the different parts of the Alps (Durand et al., 2009a) will probably be qualitatively preserved in the future.

#### 4.4 Changes in snow water equivalent

Figure 12 shows maps of the relative change in winter snow water equivalent (SWE) and the standard deviation at 1800 m a.s.l. for the different scenarios with respect to current SWE (Fig. 6b). The current decreasing trend in snow cover over recent decades reported by D09a seems to continue in the future, for all massifs and scenarios. In the B1 scenario, the decrease in SWE is significantly less than for the other two scenarios, particularly in the northern massifs (Fig. 12, upper panels). In consequence, only at the end of the century do SWE losses in the B1 scenario reach levels simulated for the earlier period in the A1B and A2 scenarios. Moreover, at the end of the century, the expected decrease under the worst case A2 scenario is about twice that projected for the B1 scenario in the Alps, and even more when only the Northern and Central Alps are considered. The impact of climate change results in a dramatic reduction of SWE, close to 100% in the southernmost massifs in the A2 scenario, and to a strong north-south SWE gradient in all scenarios.

Relative SWE changes with altitude for the different regions of the Alps are shown in Fig. 13, which suggest a strong altitudinal gradient in the SWE reduction. In the Northern Alps, under B1 conditions, the mean SWE at 1500 m a.s.l. is likely to decrease by an average of 30% for 2021–2050 and 55% for 2071–2100. These ratios increase to respectively 50% and 80% for scenario A2. At 2100 m a.s.l., mean decreases in

## Statistical adaptation of ALADIN RCM

M. Rousselot et al.

Title Page

Abstract

Introduction

Conclusions

References

Tables

Figures

◀

▶

◀

▶

Back

Close

Full Screen / Esc

Printer-friendly Version

Interactive Discussion



SWE of 20% and 30% are simulated for the B1 and A2 scenarios respectively, for 2021–2050. During this period, areas above this altitude are relatively less affected by climate warming, with average decreases in SWE varying by about 10% and 25% for the B1 and A2 scenarios, respectively. At the end of the century, this critical altitude seems to rise to 2400 m a.s.l. for the B1 scenario and higher for the other ones, in the Northern Alps.

Thus, future SWE reduction seems to significantly affect all massifs of the Alps for all scenarios at the end of the century. In particular, for this period, warming may have extremely strong impact at altitudes below 2400 m a.s.l. and preferentially in the southernmost massifs. Thus snow pack may become extremely sparse in the extreme Southern Alps in the A2 scenario.

## 5 Discussion

In this study, we have developed a procedure for adapting climate scenarios to snow modelling. This procedure consists of a statistical adaptation of fine-scale RCM fields to the alpine region. In particular, the method performs an analogue search based on minimizing a simple statistical distance between atmospheric fields of T2m, Z500 and derived from Z500 of the RCM ALADIN and the ERA40 data. The date of the selected ERA40 day is subsequently used to identify the corresponding detailed meteorological situation analysed by SAFRAN over the Alps for that day, available from a previous work (D09a). It is thus assumed that, despite the few atmospheric fields considered here, both large-scale and near-surface processes of the meteorological situation can be characterized with sufficient detail in the analogue method.

The first step of the validation indicated that both the chosen atmospheric fields and the simple statistical criterion were suitable to reconstruct current D09a climatology when a cross analogue search was applied to two distinct ERA40 datasets. The second step of the validation, where analogues were sought between ERA40 and ALADIN fields, suggested that the method tends to underestimate precipitation compared to

### Statistical adaptation of ALADIN RCM

M. Rousselot et al.

Title Page

Abstract

Introduction

Conclusions

References

Tables

Figures

◀

▶

◀

▶

Back

Close

Full Screen / Esc

Printer-friendly Version

Interactive Discussion



current climatology, mainly in summer and, to a lesser extent, in autumn. This underestimation probably reflects differences in parametrization of physical processes and topography between the ECMWF and ALADIN models.

The introduction of a statistical q-q correction provided a partial solution to this problem. This kind of correction has many advantages as it keeps some consistency between variables and can account for the annual cycle as it is applied to individual seasons separately. However, an important issue concerning this kind of correction, which is common to many other downscaling studies (Martin et al., 1997; Kallache et al., 2011), is the question of its validity in the future, despite climate change. The underlying idea is that, since the relative frequency of weather types might change in a changing climate, the resulting weather variable distribution may change. This would potentially invalidate the correction function, unless it was done for each regime separately. In our case, the analysis of weather type frequencies between present and future climate indicates that there is no important change between present and future in the frequency of weather types responsible for large precipitation events. Thus, even if this consideration does not validate the correction, it does not rule it out.

Other assumptions are that the statistical relationship between the RCM predictors and the local variables will be the same in the future, that the selected RCM predictors capture the effect of global warming, and that realistic future meteorological situations are contained in the D09a analogues dataset. These assumptions cannot be verified. Nevertheless, we have verified a posteriori that our method provides results in agreement with characteristic features of climate changes obtained at larger scale by fully dynamical methods.

Despite these limitations, the method presents several advantages. First, there is a certain added value provided by fine-scale (12 km) RCM scenarios in contrast to larger-scale scenarios, as the RCM simulations give results on several grid points over the alpine domain, and at an hourly time step for 30 yr. Thus, it is likely that fine-scale RCM outputs describe the alpine climate in terms of spatial and temporal variability with more accuracy than outputs at coarser resolution. A perspective for this work will

**Statistical adaptation  
of ALADIN RCM**

M. Rousselot et al.

[Title Page](#)[Abstract](#)[Introduction](#)[Conclusions](#)[References](#)[Tables](#)[Figures](#)[◀](#)[▶](#)[◀](#)[▶](#)[Back](#)[Close](#)[Full Screen / Esc](#)[Printer-friendly Version](#)[Interactive Discussion](#)

**Statistical adaptation  
of ALADIN RCM**

M. Rousselot et al.

[Title Page](#)[Abstract](#)[Introduction](#)[Conclusions](#)[References](#)[Tables](#)[Figures](#)[◀](#)[▶](#)[◀](#)[▶](#)[Back](#)[Close](#)[Full Screen / Esc](#)[Printer-friendly Version](#)[Interactive Discussion](#)

nevertheless be to quantify the influence of the RCM output resolution used on the quality of the scenarios obtained at the massif scale. Second, this method, which is computationally efficient compared to other analogue methods as it uses only a limited number of atmospheric and statistical parameters, provides detailed climate scenarios.

5 These scenarios are composed of daily SAFRAN fields which not only provide a full set of meteorological data but also account for massif, slope, altitude and exposition. These parameters are essential for the running of a physically elaborate snow model such as CROCUS. The spatial and daily coherence of the downscaled variables, guaranteed by the use of the SAFRAN fields, is important for the snow applications considered here because it determines the effect of climate on the snow mantle as integrated in time and allows the identification of regional patterns in the snow cover evolution. Finally, using a complex snow model such as CROCUS rather than a simple degree-day model presents several advantages. It allows computation of SWE within the snow pack, as presented in this study. Also, the physical parametrization of CROCUS takes some non-linear feedbacks of climate warming into account that accelerate the snow melt, such as temperature increase within the snowpack, which comes closer to the melting point, or the change in albedo due to changes in snow grain shapes.

10 Apart from the expected biases of the RCM inputs, which have been corrected, and the inherent uncertainty resulting from the nature of the data used for validation and the downscaling procedure, snowpack simulated in the reference situation adequately reflects current snowpack climatology. Our projections are in agreement with numerous previous studies, which underline the likelihood of a marked decrease of the snow cover in temperate regions over the coming decades (Martin and Etchevers, 2005; López et al., 2009). Our results provide further insight into the possible reasons for this SWE reduction, suggesting that simulated SWE reduction may primarily be a result of warming in all seasons, particularly from autumn to April, and possibly of a reduction of precipitation in autumn. In particular, rising temperatures may cause SWE reduction for two reasons: (i) above a given temperature threshold, precipitation falls as rain instead of snow during the snow season (extended winter, running from November to April);

(ii) rising near-surface temperatures are indicative of increased surface temperatures, which favour earlier melt of the snow cover, especially in spring. Moreover, significant SWE changes are identifiable, according to the GHG scenario, from 2021–2051, a period for which the climate response is only slightly dependent on the scenario, stressing the strong sensitivity of snow cover to small climate variations. Regions where current mean seasonal temperatures are only slightly negative are particularly sensitive to the simulated SWE reduction, and concern low to mid altitudes and the Southern and Extreme Southern Alps.

## 6 Conclusions

The aim of this study was to evaluate the potential impact of global change on snow cover in the French Alps for the forthcoming decades. Changes were evaluated by a statistical adaptation method where an analogue method was applied to high resolution RCM predictors and provided complete, physically coherent climate series suitable for snow modelling. The focus was on the validation of the method and changes in temperature, precipitation and SWE. The changes were assessed by comparing climate and snowpack simulations for the control period (1961–1990) and those of three contrasted GHG emission scenarios, for the periods 2021–2050 and 2071–2100. Special attention was paid to the detection of both seasonal and spatial changes.

The results of the validation step show that the method reproduces some features of the observed current climate with good confidence, except for summer precipitation, which is underestimated. These deviations, which should not have significant impact on snowpack modelling, were nevertheless corrected statistically.

The methodology used here seems well suited to addressing the large topographic heterogeneities and generally sparse nature of the available observational dataset that characterize mountain regions. Detailed climate scenarios have been produced, which force a complex snow model. The main conclusions drawn from an analysis of the results are as follows:

## Statistical adaptation of ALADIN RCM

M. Rousselot et al.

Title Page

Abstract

Introduction

Conclusions

References

Tables

Figures

◀

▶

◀

▶

Back

Close

Full Screen / Esc

Printer-friendly Version

Interactive Discussion



- Different GHG scenarios lead to marked differences in climate response for the 2071–2100 period, but earlier (2021–2050) for the snow response.
- Noticeable spatial differences in the magnitude of simulated changes in snow pack are detected. Snowpack in the Southern and Extreme Southern areas is clearly the most strongly affected by climate changes.
- The impact of climate change on snowpack is highly sensitive to altitudinal gradient, with significant SWE reduction at altitudes below 2000–2300 m a.s.l. in all massifs.

The question of the uncertainty has been assessed here in a preliminary manner by considering different emission scenarios. This analysis needs to be completed, ideally by considering every step in the modelling process that may introduce uncertainty: the emission scenario, as dealt with here, the global forcing from the GCM, the RCM and the resolution of its predictors, the adaptation method, and the snow model. Some of these aspects will be treated in a future study. Improvements of the method will involve consideration of more large-scale fields, which were not available from ALADIN but that will be obtained from other RCMs. Although the method seems to reproduce mean current climatological values satisfactorily, the adequate representation of temporal variability is not guaranteed. The limited number of parameters selected to compute the statistical distance (Z500, T2m and derived fields) are probably not suitable to represent the whole variety of weather phenomena. In particular, our method is not suited to addressing extreme climate events, which should therefore be treated with appropriate statistical tools (e.g. the extreme value theory, Coles, 2004).

**Statistical adaptation of ALADIN RCM**

M. Rousselot et al.

<a href="#">Title Page</a>	
<a href="#">Abstract</a>	<a href="#">Introduction</a>
<a href="#">Conclusions</a>	<a href="#">References</a>
<a href="#">Tables</a>	<a href="#">Figures</a>
<a href="#">◀</a>	<a href="#">▶</a>
<a href="#">◀</a>	<a href="#">▶</a>
<a href="#">Back</a>	<a href="#">Close</a>
<a href="#">Full Screen / Esc</a>	
<a href="#">Printer-friendly Version</a>	
<a href="#">Interactive Discussion</a>	



Discussion Paper | Discussion Paper | Discussion Paper | Discussion Paper

*Acknowledgements.* We acknowledge support by the SCAMPEI national project funded through grant ANR-08-VULN-0009-01. This research was partially funded under the EU/FP7 project ACQWA (FP7-ENV-2007-1-212250).



The publication of this article is financed by CNRS-INSU.

## References

- Acquaotta, F., Fratianni, S., Cassardo, C., and Cremonini, R.: On the continuity and climatic variability of the meteorological stations in Torino, Asti, Vercelli and Oropa, *Meteorol. Atmos. Phys.*, 103, 279–287, 2009. 173
- Alpert, P., Krichak, S. O., Shafir, H., Haim, D., and Osetinsky, I.: Climatic trends to extremes employing regional modeling and statistical interpretation over the E. Mediterranean, *Global Planet. Change*, 63(2–3), 163–170, doi:10.1016/j.gloplacha.2008.03.003, 2008. 181
- Beniston, M.: Climatic change in mountain regions: a review of possible impacts, *Theor. Appl. Climatol.*, 74(1–2), 19–31, doi:10.1007/s00704-002-0709-1, 2003.
- Beniston, M., Keller, F., and Goyette, S.: Snow pack in the Swiss Alps under changing climatic conditions: an empirical approach for climate impacts studies, *Climatic Change*, 59, 5–31, 2003. 173
- Boé, J., Terray, L., Habets, F., and Martin, E.: Statistical and dynamical downscaling of the Seine basin climate for hydro-meteorological Fstudies, *Int. J. Climatol.*, 27(12), 1643–1655, doi:10.1002/joc.1602, 2007. 181
- Boé, J., Terray, L., Martin, E., and Habets, F.: Projected changes in components of the hydrological cycle in French river basins during the 21st century, *Water Resour. Res.*, 45, W08452, doi:10.1029/2008WR007437, 2009. 182
- Brun, E., Martin, E., Simon, V., Gendre, C., and Coléou, C.: An energy and mass model of

## Statistical adaptation of ALADIN RCM

M. Rousselot et al.

Title Page

Abstract

Introduction

Conclusions

References

Tables

Figures

◀

▶

◀

▶

Back

Close

Full Screen / Esc

Printer-friendly Version

Interactive Discussion



**Statistical adaptation  
of ALADIN RCM**

M. Rousselot et al.

Title Page

Abstract

Introduction

Conclusions

References

Tables

Figures

◀

▶

◀

▶

Back

Close

Full Screen / Esc

Printer-friendly Version

Interactive Discussion



snow cover suitable for operational avalanche forecasting, *J. Glaciol.*, 35(121), 333–342, 1989. 177

Brun, E., David, P., Sudul, M., and Brugnot, G.: A numerical model to simulate snow cover stratigraphy for operational avalanche forecasting, *J. Glaciol.*, 38(128), 13–22, 1992. 177

5 Bubnová, R., Hello, G., Bénard, P., and Geleyn, J. F.: Integration of the fully elastic equations cast in the hydrostatic pressure terrain-following coordinate in the framework of ARPEGE/Aladin NWP system, *Mon. Weather Rev.*, 123, 515–535, 1995. 175

Christensen, J. H., and Christensen, O. B.: A summary of the PRUDENCE model projections of changes in European climate by the end of this century, *Climatic Change*, 81(1), 7–30, doi:10.1007/s10584-006-9210-7, 2007. 174

10 Coles, S.: An Introduction to Statistical Modeling of Extreme Values, 3rd edn., Springer Series in Statistics, Springer-Verlag, London, 2004. 190

Colin, J., Déqué, M., Radu, R., and Somot, S.: Sensitivity study of heavy precipitation in Limited Area Model climate simulations: influence of the size of the domain and the use of the spectral nudging technique, *Tellus*, 62(5), 591–604. doi:10.1111/j.1600-0870.2010.00467.x., 2010. 176

Déqué, M.: Frequency of precipitation and temperature extremes over France in an anthropogenic scenario: model results and statistical correction according to observed values, *Global Planet. Change*, 57, 16–26, 2007. 177, 181

20 Déqué, M., and Somot, S.: Added value of high resolution for ALADIN Regional Climate Model, *Időjárás Quat. J. Hungarian Met. Service*, 112(3-4), 179–190, 2008. 174, 176

Durand, Y., Brun, E., Mérindol, L., Guyomarch, G., Lesaffre, B., and Martin, E.: A meteorological estimation of relevant parameters for snow models, *Ann. Glaciol.*, 18, 65–71, 1993. 179

25 Durand, Y., Giraud, G., Brun, E., Mérindol, L., and Martin, E.: A computer-based system simulating snowpack structures as a tool for regional avalanche forecasting, *J. Glaciol.*, 45(151), 469–484, 1999. 177

Durand, Y., Laternser, M., Giraud, G., Etchevers, P., Lesaffre, B., and Mérindol, L.: Reanalysis of 44 years of climate in the French Alps (1958–2002): methodology, model validation, climatology and trends for air temperature and precipitation, *J. Appl. Meteorol. Clim.*, 48(3), 429–449, doi:10.1175/2008JAMC1808.1, 2009a. 173, 176, 180, 183, 184, 185

30 Durand, Y., Giraud, G., Laternser, M., Etchevers, P., Mérindol, L., and Lesaffre, B.: Reanalysis of 47 years of climate in the French Alps (1958–2005): climatology and trends for snow

**Statistical adaptation  
of ALADIN RCM**

M. Rousselot et al.

Title Page

Abstract

Introduction

Conclusions

References

Tables

Figures

◀

▶

◀

▶

Back

Close

Full Screen / Esc

Printer-friendly Version

Interactive Discussion



cover, *J. Appl. Meteorol. Clim.*, 48(12), 2487–2512, doi:10.1175/2009JAMC1810.1, 2009b. 173, 178, 182

ECMWF, ERA-40: ECMWF 45-years reanalysis of the global atmosphere and surface conditions 1957–2002, *ECMWF Newsletter*, 101 – Summer-Autumn 2004, Shinfield Park, Reading, Berkshire, RG29AX, UK, 2004. 176

Farda, A., Déqué, M., Somot, S., Horányi, A., Spiridonov, V., and Tóth, H.: Model Aladin as regional climate model for Central and Eastern Europe, *Stud. Geophys. Geod.*, 54, 313–332, 2010. 174

Frei, C. and Schär, C.: A precipitation climatology of the Alps from high-resolution rain-gauge observations, *Int. J. Climatol.*, 18(8), 873–900, doi:10.1002/joc255, 1998. 173

Frey-Buness, F., Heimann, D., and Sausen, R.: A statistical-dynamical downscaling procedure for global climate simulations, *Theor. Appl. Climatol.*, 50(3–4), 117–131, 1995. 174

Gibelin, A. L. and Déqué, M.: Anthropogenic climate change over the Mediterranean region simulated by a global variable resolution model, *Clim. Dynam.*, 20, 327–339, 2003. 176

Hagemann, S., Machenhauer, B., Jones, R., Christensen, O. B., Déqué, M., Jacob, D., and Vidale, P. L.: Evaluation of water and energy budgets in regional climate models applied over Europe, *Clim. Dynam.*, 23, 547–567, 2004. 174

Haylock, M. R., Hofstra, N., Klein Tank, A. M. G., Klok, E. J., Jones, P. D., and New, M.: A European daily high-resolution gridded data set of surface temperature and precipitation for 1950–2006, *J. Geophys. Res.*, 113, D20119, doi:10.1029/2008JD010201, 2008. 174

Hantel, M., Ehrendorfer, M., and Haslinger, A.: Climate sensitivity of snow cover duration in Austria, *Int. J. Climatol.*, 20(6), 615–640, doi:10.1002/joc489, 2000. 173

Hewitt, C. D. and Griggs, D. J.: Ensembles-based predictions of climate changes and their impacts, *EOS T. Am. Geophys. Un.*, 85, 566, 2004. 174

Hohenegger, C., Brockhaus, P., and Schär, C.: Towards climate simulations at cloud-resolving scales, *Meteorol. Z.*, 17(4), 383–394, doi:10.1127/0941-2948/2008/0303, 2008. 174

IPCC: Climate Change 2007: The Physical Science Basis, Contribution of working group I to the fourth assessment report of the Intergovernmental Panel on Climate Change, edited by: Solomon, S., Qin, D., Manning, M., Chen, Z., Marquis, M., Averyt, K. B., Tignor, M., and Miller H. L., Cambridge University Press, Cambridge, UK and New York, NY, USA, 2007. 178, 182

Kallache, M., Vrac, M., Naveau, P., and Michelangeli, P.-A.: Non-stationary probabilistic downscaling of extreme precipitation, *J. Geophys. Res.*, 116, D05113,

**Statistical adaptation  
of ALADIN RCM**

M. Rousselot et al.

Title Page

Abstract

Introduction

Conclusions

References

Tables

Figures

◀

▶

◀

▶

Back

Close

Full Screen / Esc

Printer-friendly Version

Interactive Discussion



doi:10.1029/2010JD014892, 2011. 181, 187

Kettle, H. and Thompson, R.: Statistical downscaling in European mountains: verification of air temperature reconstructions, *Climate Res.*, 26(2), 97–112, 2004. 174

Laternser, M. and Schneebeli, M.: Long-term snow climate trends of the Swiss Alps (1931–99), *Int. J. Climatol.*, 23(7), 733–750, doi:10.1002/joc.912, 2003. 173

van der Linden, P. and Mitchell, J. F. B.: ENSEMBLES: Climate Change and its Impacts: Summary of research and results from the ENSEMBLES project, Tech. rep., Met Office Hadley Centre, FitzRoy Road, Exeter EX1 3PB, UK, 2009. 174

López-Moreno, J. I., Goyette, S., and Beniston, M.: Impact of climate change on snowpack in the Pyrenees: horizontal and spatial variability and vertical gradients, *J. Hydrol.*, 374, 384–396, doi:10.1016/j.jhydrol.2009.06.049, 2009. 188

Mahalanobis, P. C.: On the generalised distance in statistics, *P. Natl Instit. Sci. India*, 2(1), 49–55, 1936. 177

Maraun, D., Wetterhall, F., Ireson, A. M., Chandler, R. E., Kendon, E. J., Widmann, M., Brienen, S., Rust, H. W., Sauter, R., Theme, M., Venema, V. K. C., Chun, K. P., Goodess, C. M., Jones, R. G., Onof, C., Vrac, M., and Thiele-Eich, I.: Precipitation downscaling under climate change: recent developments to bridge the gap between dynamical models and the end user, *Rev. Geophys.*, 48(3), RG3003, doi:10.1029/2009RG000314, 2010b. 173, 174

Martin, E. and Etchevers, P.: Impact of climatic changes on snow cover and snow hydrology in the French Alps, *Adv. Glob. Change Res.*, 23(II), 235–242, 2005. 173, 188

Martin, E., Brun, E., and Durand, Y.: Sensitivity of the French Alps snow cover to the variation of climatic variables, *Ann. Geophys.*, 12, 469–477, doi:10.1007/s00585-994-0469-6, 1994. 173

Martin, E., Timbal, B., and Brun, E.: Downscaling of general circulation model outputs: simulation of the snow climatology of the French Alps and sensitivity to climate change, *Clim. Dynam.*, 13, 45–56, 1997. 173, 174, 187

Radu, R., Déqué, M., and Somot, S.: Spectral nudging in a spectral regional climate model, *Tellus A*, 60, 885–897, 2008. 175

Schmidli, J., Goodess, C. M., Frei, C., Haylock, M. R., Hündecha, Y., Ribalaygua, J., and Schmith, T.: Statistical and dynamical downscaling of precipitation: An evaluation and comparison of scenarios for the European Alps, *J. Geophys. Res.*, 112, D04105, doi:10.1029/2005JD007026, 2007. 174

Schöner, W., Auer, I., and Böhm R.: Climate variability and glacier reaction in the Austrian Eastern Alps, *Ann. Glaciol.*, 31(1), 31–38, 2000. 173

Terray, L., Demory, M. E., Déqué, M., de Coetlogon, G., and Maisonnavé, E.: Simulation of late twenty-first century changes in wintertime atmospheric circulation over Europe due to anthropogenic causes, *J. Climate*, 17, 4630–4635, 2004. 182

5

TCD

6, 171–210, 2012

## Statistical adaptation of ALADIN RCM

M. Rousselot et al.

Title Page

Abstract

Introduction

Conclusions

References

Tables

Figures

⏪

⏩

◀

▶

Back

Close

Full Screen / Esc

Printer-friendly Version

Interactive Discussion



**Statistical adaptation  
of ALADIN RCM**

M. Rousselot et al.

Title Page

Abstract

Introduction

Conclusions

References

Tables

Figures

I◀

▶I

◀

▶

Back

Close

Full Screen / Esc

Printer-friendly Version

Interactive Discussion

**Table 1.** Origin of T2m and Z500 datasets used for the analogue search in the CT and CR experiments.

CT	ERA40	ERA40
CR	ALADIN	ERA40

**Table 2.** Comparison of annual T2m (°C) and precipitation (mm d<sup>-1</sup>) means and standard deviation over the Alps in the CT experiment and the D09a climatology, and the differences between the mean values obtained in the two experiments.

Massif	CT				D09a				Differences of means (CT-D09a)	
	T2m		Precipitation		T2m		Precipitation		T2m	Precipitation
	Mean	$\sigma$	Mean	$\sigma$	Mean	$\sigma$	Mean	$\sigma$		
Chablais	3.26	0.58	4.59	0.97	3.09	0.55	5.16	0.80	0.17	-0.57
Aravis	3.37	0.57	4.84	1.04	3.19	0.57	5.45	0.87	0.18	-0.61
Bauges	3.45	0.58	4.43	1.03	3.20	0.58	5.02	0.98	0.25	-0.59
Chartreuse	3.65	0.59	4.71	1.01	3.38	0.61	5.41	0.84	0.27	-0.70
Vercors	3.73	0.58	3.76	0.79	3.50	0.64	4.35	0.68	0.23	-0.59
Mont Blanc	3.33	0.55	4.33	0.90	3.22	0.55	4.91	0.77	0.11	-0.58
Beaufortain	3.53	0.57	3.98	0.92	3.39	0.56	4.56	0.79	0.14	-0.58
Haute-Tarentaise	3.52	0.56	2.83	0.66	3.48	0.54	3.27	0.64	0.04	-0.44
Haute Maurienne	3.69	0.55	2.42	0.58	3.69	0.52	2.86	0.64	0	-0.44
Vanoise	3.58	0.56	2.82	0.69	3.50	0.52	3.24	0.58	0.08	-0.42
Maurienne	3.70	0.57	3.19	0.76	3.55	0.55	3.63	0.62	0.15	-0.44
Belledonne	3.66	0.57	4.22	0.94	3.46	0.56	4.80	0.74	0.20	-0.58
Grandes Rousses	3.75	0.57	3.11	0.79	3.62	0.55	3.49	0.66	0.13	-0.38
Thabor	3.80	0.56	2.30	0.58	3.76	0.54	2.65	0.57	0.04	-0.35
Oisans	3.86	0.56	3.30	0.76	3.77	0.58	3.68	0.67	0.09	-0.38
Pelvoux	3.99	0.56	2.96	0.74	3.97	0.56	3.31	0.72	0.02	-0.35
Champsaur	4.06	0.56	3.04	0.68	4.03	0.59	3.34	0.66	0.03	-0.30
Dévoluy	3.92	0.57	2.94	0.63	3.82	0.63	3.26	0.64	0.10	-0.32
Queyras	4.01	0.56	1.93	0.47	4.04	0.53	2.23	0.45	-0.03	-0.30
Parpaillon	4.34	0.55	2.30	0.55	4.39	0.52	2.57	0.47	-0.05	-0.27
Ubaye	4.58	0.55	2.27	0.51	4.61	0.52	2.52	0.54	-0.03	-0.25
Alpes Azur�ennes	4.83	0.55	2.92	0.73	4.83	0.52	3.22	0.68	0	-0.30
Mercantour	4.84	0.52	3.25	0.88	4.92	0.47	3.62	0.82	-0.08	-0.37

Title Page

Abstract Introduction

Conclusions References

Tables Figures

◀ ▶

◀ ▶

Back Close

Full Screen / Esc

Printer-friendly Version

Interactive Discussion



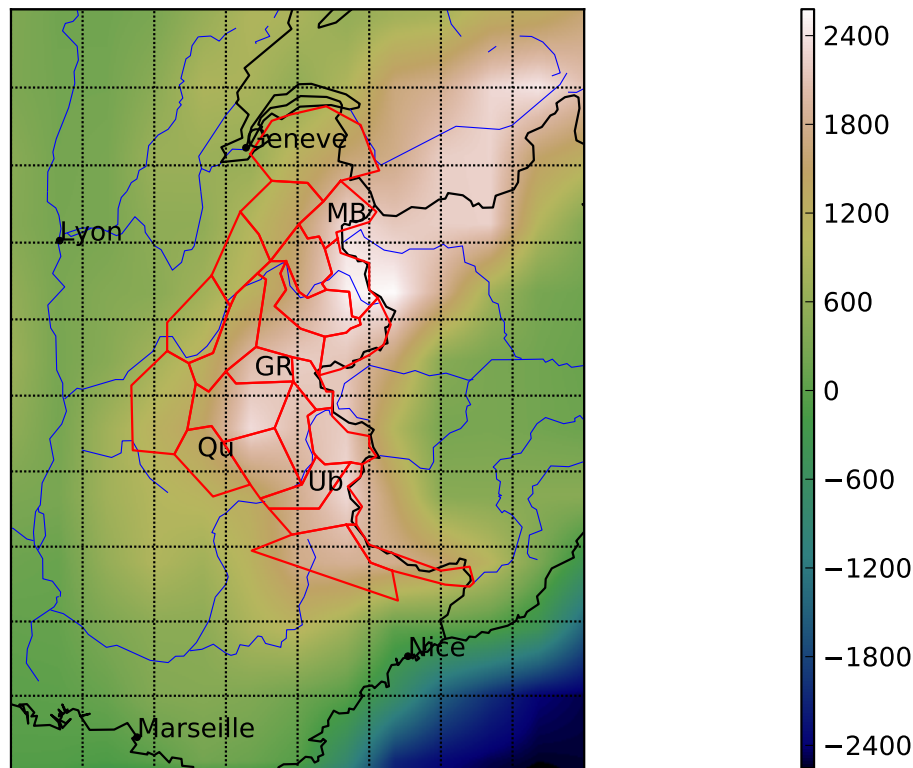


**Fig. 1.** Map showing surface elevation of the domain and the grid used for the analogue research with the 23 massifs of the French Alps as defined in SAFRAN (red line, see text for details). MB, GR, Qu and Ub designate the Mont-Blanc, Grandes Rousses, Queyras and Ubaye massifs, respectively.

**Statistical adaptation of ALADIN RCM**

M. Rousselot et al.

Title Page

Abstract Introduction

Conclusions References

Tables Figures

◀ ▶

◀ ▶

Back Close

Full Screen / Esc

Printer-friendly Version

Interactive Discussion



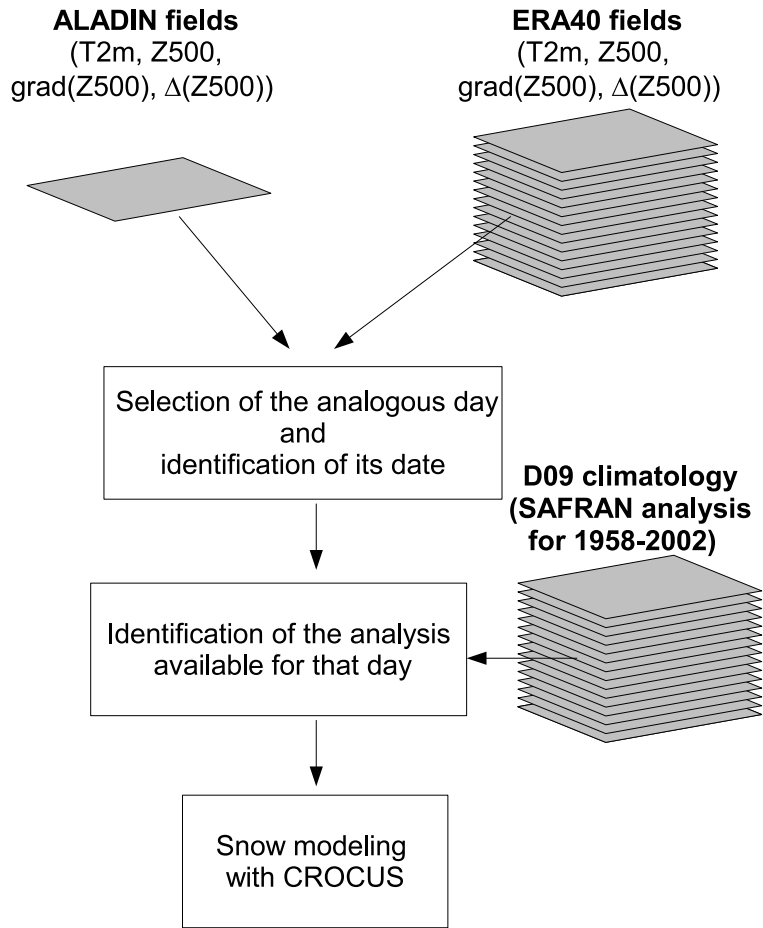


**Fig. 2.** Schematic diagram of the method, from analogues selection to snow modelling.

Title Page	
Abstract	Introduction
Conclusions	References
Tables	Figures
◀	▶
◀	▶
Back	Close
Full Screen / Esc	
Printer-friendly Version	
Interactive Discussion	



Type	Pressure fields	Syn. flows	Precipitation on the Alps
1	Low, flat gradient over France	S or N	Light - moderate
2	Low, on the Northern Alps	SW	Light - heavy
3	Through along Slovakia/Baltic/Sea axis	N-NW	Light - heavy
4	Low, on Scotland and Sweden	W-NW	Heavy
5	High on the Alps, low gradients	SW	None - moderate
6	Low, along Italy/Scandinavia axis	S or N	Light - moderate
7	High and stable	Weak	None - light

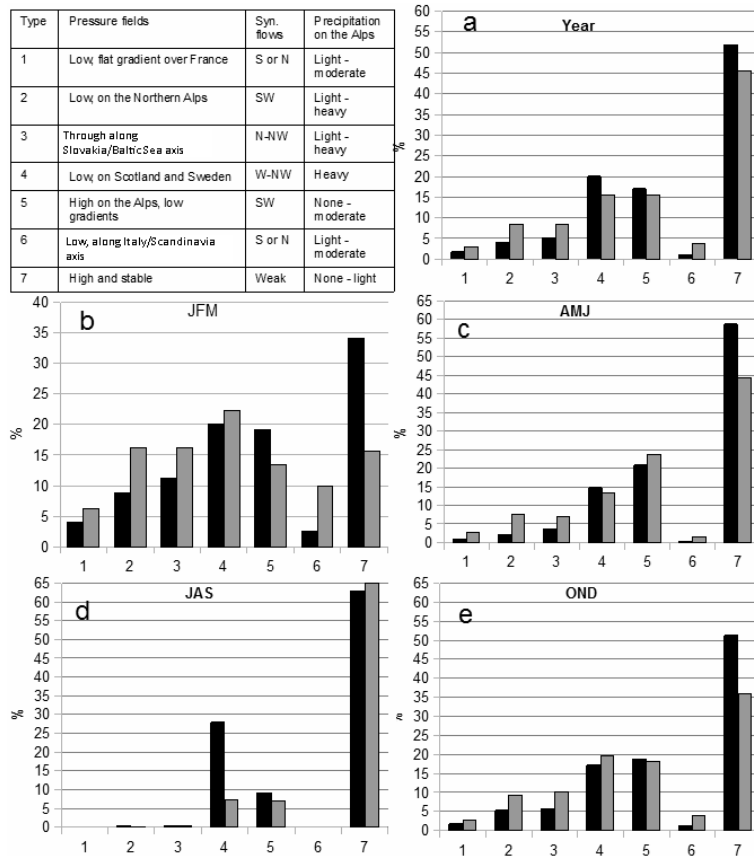


**Fig. 3.** Comparison of weather type frequencies over the French Alps derived from the D09a climatology (black) and the CT experiment (grey) for 1961–1990, with (a) annual and (b–e) seasonal distributions. The inset table summarizes SAFRAN classification of weather types.

Statistical adaptation of ALADIN RCM

M. Rousselot et al.

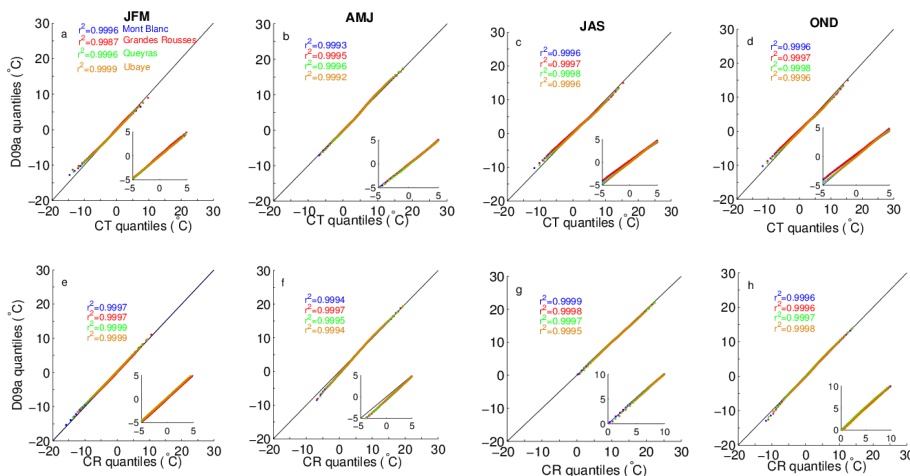


**Fig. 4.** Seasonal T2m quantile-quantile diagrams (°C) obtained in the (a–d) CT and (e–h) CR experiments at 1800 m a.s.l. for the Mont-Blanc (blue), Grandes Rousses (red), Queyras (green) and Ubaye (orange) massifs (see Fig. 1 for location).  $r^2$  is the correlation coefficient between the simulated and D09a quantiles for each massif. Insets show zooms.

Title Page

Abstract Introduction

Conclusions References

Tables Figures

◀ ▶

◀ ▶

Back Close

Full Screen / Esc

Printer-friendly Version

Interactive Discussion



Statistical adaptation  
of ALADIN RCM

M. Rousselot et al.

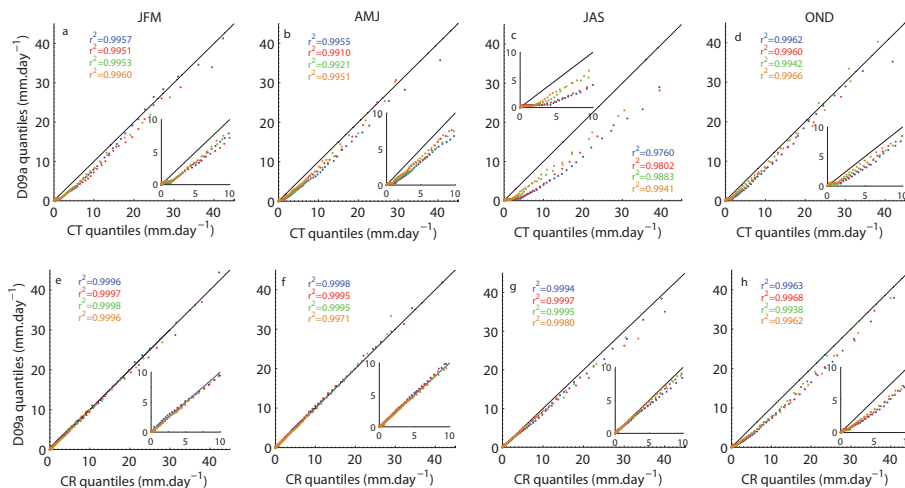


Fig. 5. Same as Fig. 4, but for precipitation.

Title Page

Abstract

Introduction

Conclusions

References

Tables

Figures

◀

▶

◀

▶

Back

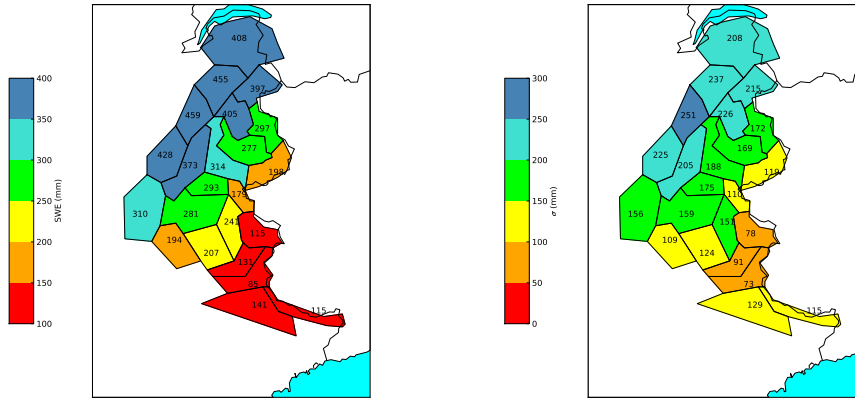
Close

Full Screen / Esc

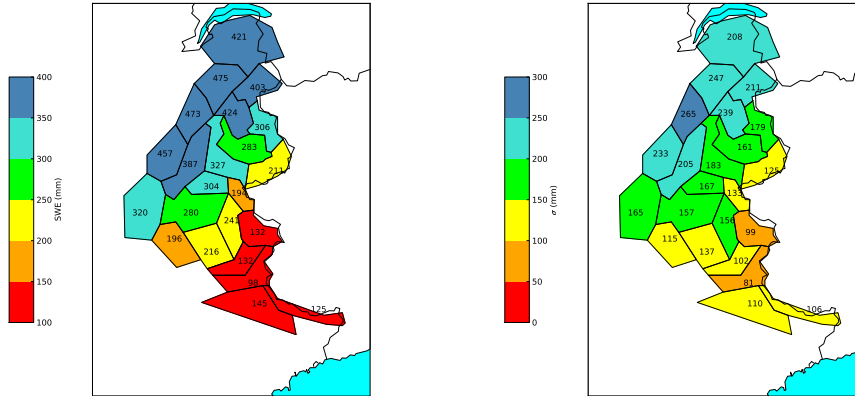
Printer-friendly Version

Interactive Discussion





a



b

**Fig. 6.** Mean winter (JFM) values (left) and standard deviation (right) of the snow water equivalent (SWE) at 1800 m a.s.l. for **(a)** the CT experiment and **(b)** D09b climatology, for 1961–1990.

## Statistical adaptation of ALADIN RCM

M. Rousselot et al.

Title Page

Abstract

Introduction

Conclusions

References

Tables

Figures

◀

▶

◀

▶

Back

Close

Full Screen / Esc

Printer-friendly Version

Interactive Discussion

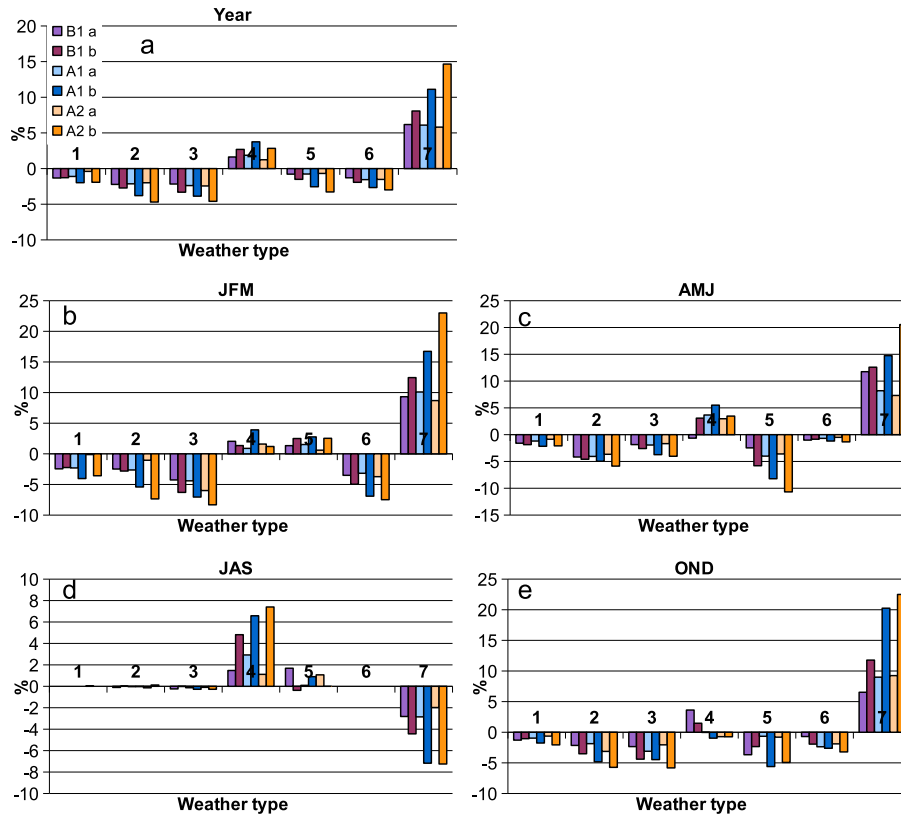


**Fig. 7.** Changes in % in weather type annual and seasonal frequency over the French Alps for the periods 2021–2050 and 2071–2100 (subscripts a and b, respectively) with respect to frequencies simulated for the period 1961–1990 (CT experiment, see Fig. 2), for different scenarios (B1, A1 and A2). The weather type classification is the same as for Fig. 2.

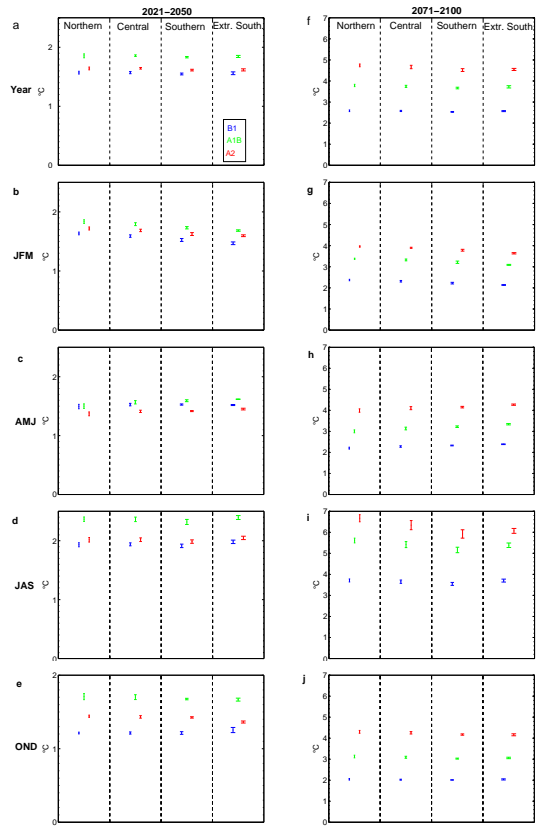


**Fig. 8.** Changes in (a) annual and (b–e) seasonal mean T2m at 1800 m a.s.l. over the Northern, Central, Southern and Extreme Southern French Alps, for the scenarios B1 (blue), A1 (green) and A2 (red) and for the periods 2021–2050 (left panels) and 2071–2100 (right panels) with respect to results of the CT experiment. The error bars indicate standard deviation.

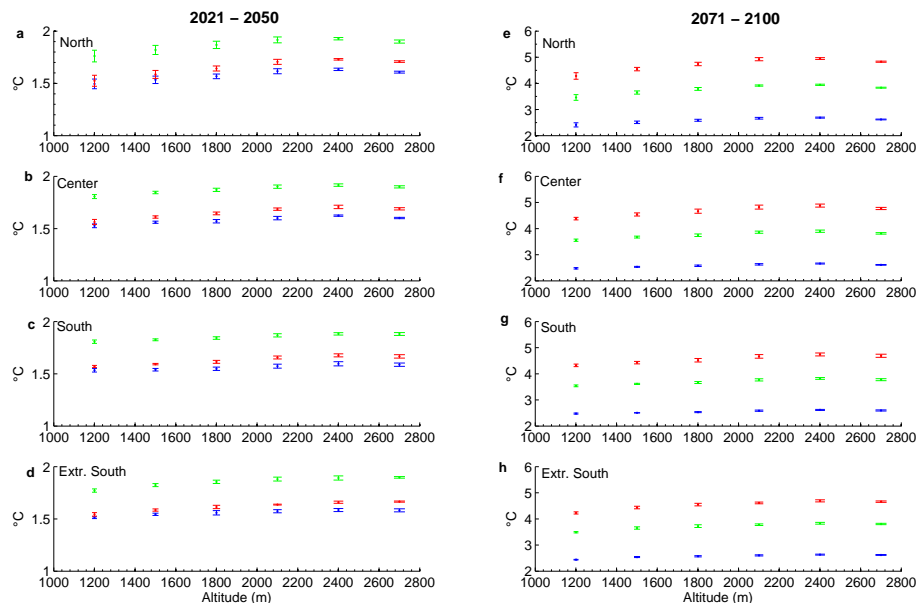


**Fig. 9.** Changes in (a) annual mean T2m as a function of altitude over the (a and b) Northern, (c and d) Central, (e and f) Southern and (g and h) Extreme Southern French Alps, for the scenarios B1 (blue), A1 (green) and A2 (red) and the periods 2021–2050 (left panels) and 2071–2100 (right panels) with respect to results of the CT experiment. The error bars indicate standard deviation. Note the different scales.

Title Page

Abstract Introduction

Conclusions References

Tables Figures

◀ ▶

◀ ▶

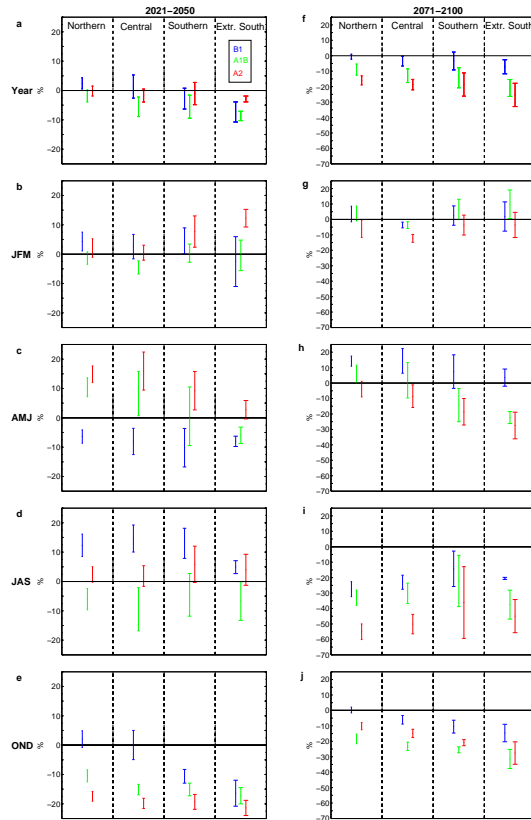
Back Close

Full Screen / Esc

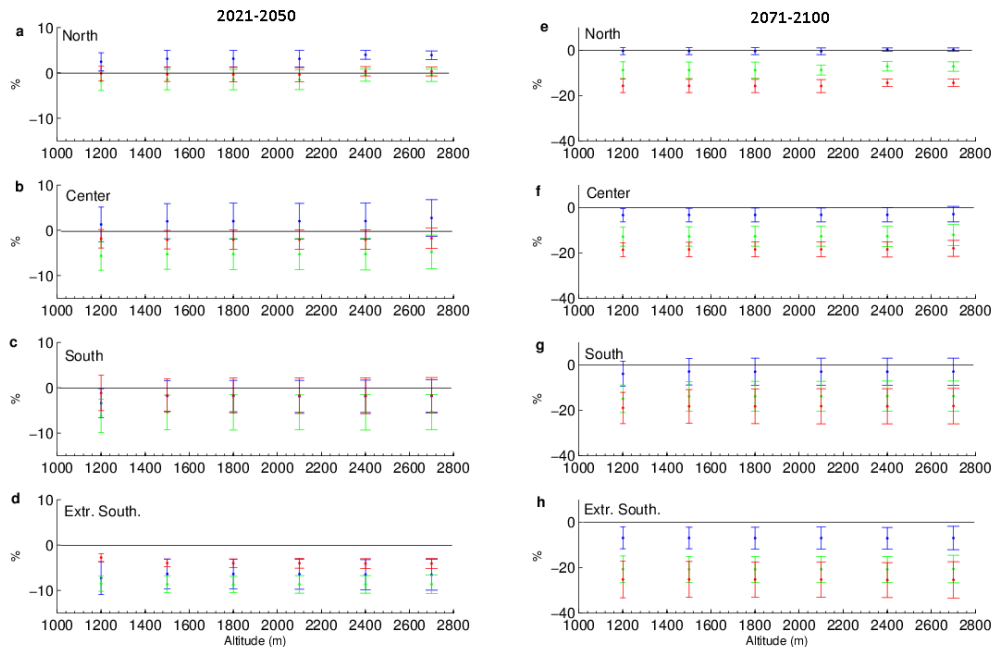
Printer-friendly Version

Interactive Discussion



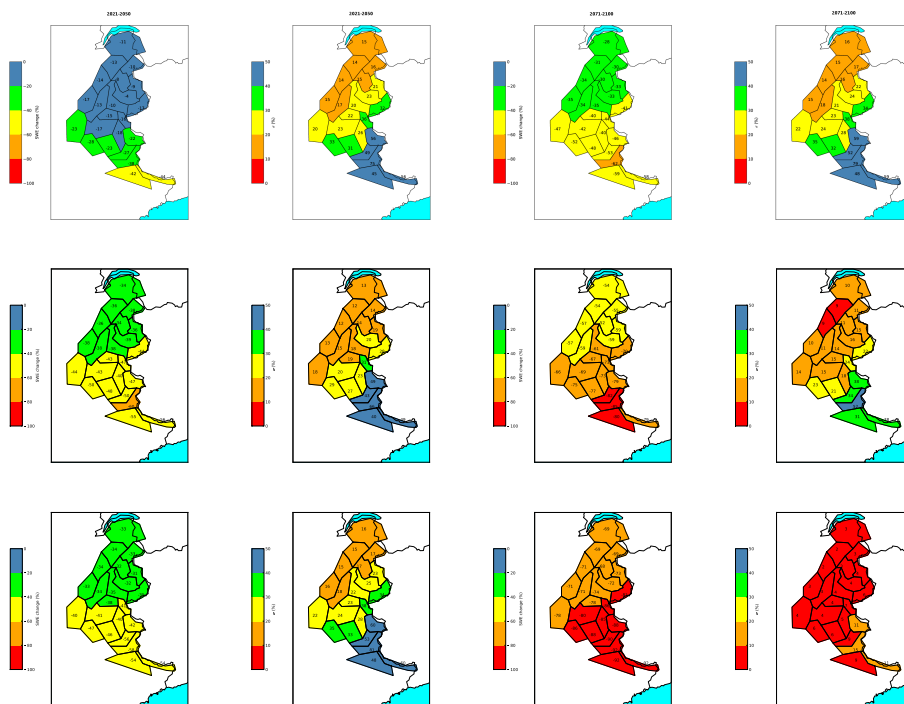


**Fig. 10.** Changes in (a) annual and (b–e) seasonal mean precipitation at 1800 m a.s.l. over the Northern, Central, Southern and Extreme Southern French Alps, for the scenarios B1 (blue), A1 (green) and A2 (red) and the periods 2021–2050 (left panels) and 2071–2100 (right panels) with respect to results of the CT experiment. The error bars indicate standard deviation.



**Fig. 11.** Changes in (a) annual mean precipitation as a function of altitude over the (a and b) Northern, (c and d) Central, (e and f) Southern and (g and h) Extreme Southern French Alps, for the scenarios B1 (blue), A1 (green) and A2 (red) and the periods 2021–2050 (left panels) and 2071–2100 (right panels) with respect to results of the CT experiment. The error bars indicate standard deviation. Note the different scales.

[Title Page](#)
[Abstract](#)
[Introduction](#)
[Conclusions](#)
[References](#)
[Tables](#)
[Figures](#)
[◀](#)
[▶](#)
[◀](#)
[▶](#)
[Back](#)
[Close](#)
[Full Screen / Esc](#)
[Printer-friendly Version](#)
[Interactive Discussion](#)

**Fig. 12.** Changes in winter snow water equivalent (%) at 1800 m a.s.l. and standard deviation over the French Alps, for the scenarios B1, A1 and A2 and the periods 2021–2050 (left panels) and 2071–2100 (right panels) with respect to results of the CT experiment.

Title Page

Abstract

Introduction

Conclusions

References

Tables

Figures

◀

▶

◀

▶

Back

Close

Full Screen / Esc

Printer-friendly Version

Interactive Discussion



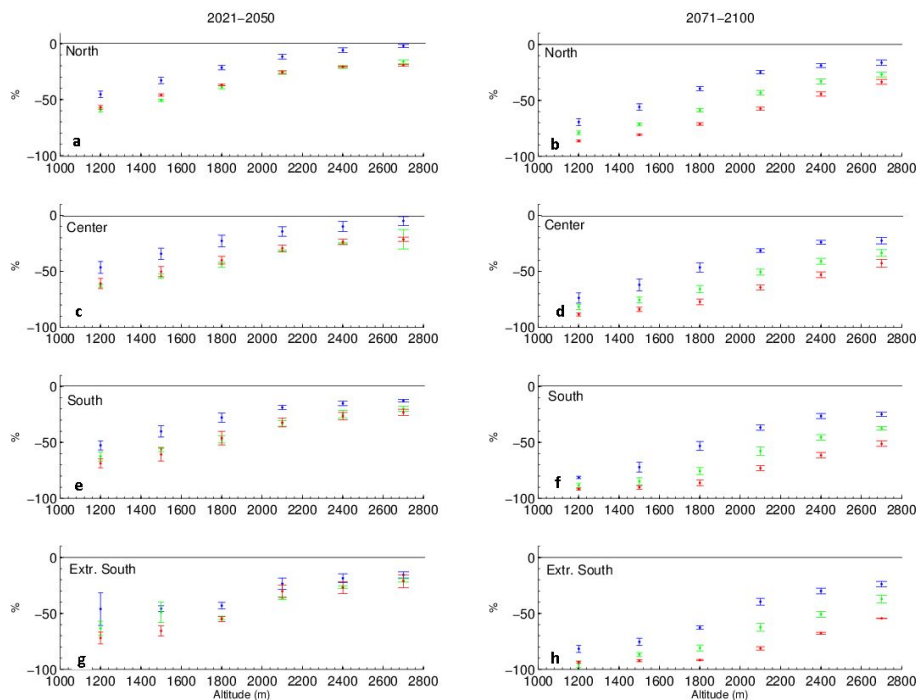


**Fig. 13.** Mean JFM snow water equivalent (%) as a function of altitude over the (a and b) Northern, (c and d) Central, (e and f) Southern and (g and h) Extreme Southern French Alps, for the scenarios B1 (blue), A1 (green) and A2 (red) and the periods 2021–2050 (left panels) and 2071–2100 (right panels). The error bars indicate standard deviation. Note the different scales.

Title Page

Abstract

Introduction

Conclusions

References

Tables

Figures

◀

▶

◀

▶

Back

Close

Full Screen / Esc

Printer-friendly Version

Interactive Discussion

